Evidence for a Percolation-Driven Transition to Coherent Surface Superconductivity

Jürgen Kötzler, Lars von Sawilski, and Sara Casalbuoni
Institut für Angewandte Physik und Zentrum für Mikrostrukturforschung, Universität Hamburg, Jungiusstrasse 11, D-20355 Hamburg, Germany
(Received 29 August 2003; published 10 February 2004)

Above the upper critical field we have investigated the field dependences of the surface conductance, $G' - iG''$, and the critical current J_c of an electropolished pure niobium cylinder. The low frequency limits of G', G'', and J_c display power-law singularities, defining a transition to coherent surface superconductivity at H_{c3}^c. The critical exponents as well as the dynamical scaling of $G' - iG''$ are consistent with predictions for a two-dimensional percolation transition. Relating H_{c3}^c to the conventional onset field, we find $H_{c3}^c/H_{c3} = 0.81$, and, surprisingly, this ratio turns out to be independent of significant variations of H_{c3} due to differently structured surfaces.

DOI: 10.1103/PhysRevLett.92.067005 PACS numbers: 74.25.Op, 74.25.Bt, 74.25.Nf, 74.70.Ad

Almost four decades ago, Saint-James and de Gennes [1] discovered the nucleation of superconducting regions in a thin surface sheath in fields significantly higher than the critical magnetic field for nucleation in the volume. The famous result, $H_{c3} = 2.392\kappa H_{c,th}$, where $H_{c,th}$ is the thermodynamical critical field and κ the Ginzburg-Landau (GL) parameter, was obtained from a numerical solution of the linearized GL equations at flat vacuum-superconductor interfaces oriented parallel to the applied field H. As an immediate consequence, the onset of transport supercurrents in fields above the appearance of volume diamagnetism could be explained. Quite recently, this surface superconductivity (SSC), in particular, the case of niobium, attracted renewed interest from quite different directions [2–6]. Some basic features of SSC, e.g., the temperature variation of H_{c3}, were previously explored for this type II superconductor ($\kappa > 1/\sqrt{2}$) [7]. Specific effects of the SSC have been suggested for the paramagnetic Meissner effect of Nb disks [2], for stochastic resonances [3], and, rather spectacularly, on the formation of the vortex Bragg glass at the so-called second peak field [4] $H_p < H_{c2} = \sqrt{2}\kappa H_{c,th}$. Moreover, it has been suggested [5] to employ SSC as a tool to explore the surface treatments which improved the performance of large-scale Nb cavities for linear particle accelerators [6]. This idea is based on the fact that, for pure Nb, $\kappa = \lambda/\xi$ is in the order of unity [7], so that SSC and electromagnetic losses of the microwave fields reside in surface sheaths of the same thicknesses given by the correlation length ξ and penetration depth λ, respectively.

In this Letter we report novel basic phenomena of SSC for a Nb cylinder, which most likely are observable in all superconductors (SC's). The main result is the formation of coherent SSC at a field H_{c3}^c below the nucleation field H_{c3}. This phase transition is well characterized by power singularities of the real and imaginary parts of the electrical surface conductances G' and G'', when H_{c3}^c is approached from the normal and superconducting sides, respectively. The values of the critical exponents of G' and G'', $s = t = 1.3(1)$, agree with those predicted for percolating, two-dimensional (2D) normal-SC networks [8–10]. This percolation picture for SSC is supported by the validity of dynamic scaling for $G' - iG''$ as well as by properties of a critical surface current appearing at H_{c3}^c. The ratio $H_{c3}^c/H_{c3} = 0.81$ agrees with those of Nb cylinders with different surface topology and impurity concentration [5] which affect H_{c3} rather strongly. This feature indicates a general, yet unknown, mechanism behind the percolation transition to coherent SSC.

The present Nb cylinder has been cut from sheets [11], from which the microwave cavities for the TESLA facility are drawn [6]. The sample was subjected to the same annealing, chemical, and electrolytical surface polishing processes as the cavities. Surface images by scanning electron and atomic force microscopy [12] revealed large areas, $20 \times 20\ \mu\text{m}^2$, of low roughness, $\delta r \lesssim 1.5$ nm, which are separated by grain boundaries with slightly enhanced $\delta r's$. The magnetic moments and the complex susceptibilities $\chi' - i\chi''$ between 1 Hz and 1 kHz have been measured by a Quantum Design MPMS2. The dc and ac magnetic fields were carefully aligned parallel to the symmetry axis of the cylinder, so that above H_{c2} SSC could be nucleated only on the sides. An ac amplitude of 10 mOe proved to be sufficient to obtain the linear response shown in Fig. 1 for selected temperatures and $f = 10$ Hz. Then, $\chi(\omega)$ is related to the homogeneous ac conductivity $\sigma(\omega)$ of a cylinder of radius R [13] by the well-known relation, $\chi(\omega) = \chi_\infty[2I_0'(x)/xI_o(x) - 1]$, where χ_∞ can be measured in the Meissner state, $I_o(x)$ is the zero-order Bessel function, and $x = [i\omega R^2\mu_0\sigma(\omega)]^{1/2}$ with $\mu_0 = 4\pi \times 10^{-7}$ V s/Am. Using an inversion routine, $\sigma(\omega)$ is obtained from $\chi(\omega)$ [14]. The constant values $\chi = \chi_n$, indicated in Fig. 1, yield the "normal" conductivity σ_n from which follows a residual resistance ratio of 300 as specified by the manufacturer [11]. It is common practice (e.g., Refs. [4,7]) to define H_{c3} by the

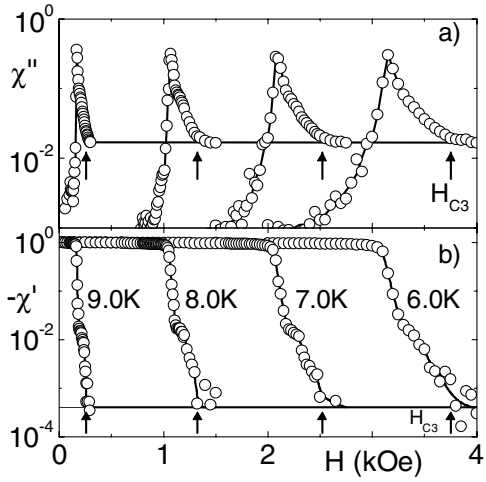

FIG. 1. (a) Imaginary and (b) real parts of the linear ac susceptibility at 10 Hz for temperatures between 6 and 9 K. The conventional nucleation fields H_{c3} (arrows) are defined by the onset of an excess absorption $\chi'' - \chi_n''$ or dispersion, $\chi' - \chi_n'$, where $\chi_n' - i\chi_n''$ (solid lines) is determined by the normal conductivity, $\sigma'(H > H_{c3}) = 2.0 \times 10^7$ S/cm.

onset of SSC, $\sigma \gtrsim \sigma_n$, which implies an excess absorption and screening; see Fig. 1.

Below the nucleation field $H_{c3}(T)$, both χ'' and $-\chi'$ rapidly increase in Fig. 1. According to Fig. 2(b), this is associated with predominantly Ohmic behavior $G_+' \gg G_-''$ [15]. Upon further reduction of the field, the relation between G' and G'' reverses, as demonstrated by the phase G''/G' in Fig. 2(a). This signals a continuous phase transition to long-range superconductivity at a *coherent* surface critical field $H_{c3}^c(T)$. In general, such a transition may be accompanied by thermal [16,17] or concentration fluctuations in a normal-SC network [8–10]. In either case and in the limit of low frequencies, the leading singularities of $G(\omega)$ on both sides of H_{c3}^c are expected to obey power laws. Above the transition, it is the diverging dc conductance, $G_+(\omega \to 0, H) = G_+(H/H_{c3}^c - 1)^{-\gamma}$, whereas below H_{c3}^c, it is the onset of the superfluid London-type response, $G_-(\omega \to 0, H) = (1 - H/H_{c3}^c)^\beta/(i\omega L_k)$. The fits, exemplified for $T = 7.0$ K in Fig. 2(b), define H_{c3}^c to an accuracy of less than 0.5% and, moreover, yield identical critical exponents, $\gamma = \beta = 1.3 \pm 0.1$. Another remarkable feature emerging from Fig. 2 is the value of the phase at H_{c3}^c, $G''/G' = 1$. Since at a SC phase transition one has $G_c(\omega, H_{c3}^c) = G_0(i\omega/\omega_0)^{-1/\delta}$ [9,14,16,17], where ω_0 is a microscopic relaxation rate, $G' = G''$ implies $\delta = 2$.

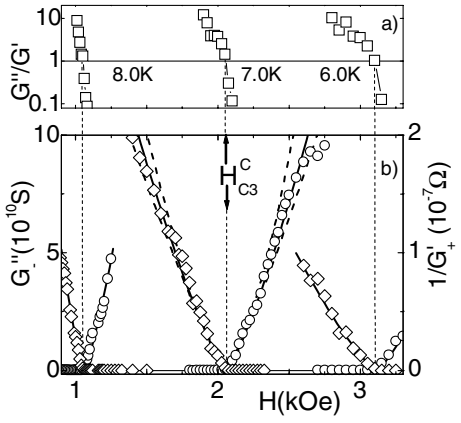

FIG. 2. (a) Phase of the 10 Hz surface conductance, showing $G'' = G'$ at H_{c3}^c. (b) Analyses of the singular behavior of G' (○) and G'' (◇) near the transitions to coherent SSC by power laws in $|1 - H/H_{c3}^c|$, which unambiguously define $H_{c3}^c(T)$ from above and below, respectively. The solid curves are the best fits with $\beta = \gamma = 1.3$. The accuracy of the exponent is illustrated by the best fits to $\beta = \gamma = 1.3 \pm 0.1$ (dashed lines).

Before discussing the exponents β, γ, and δ extracted from $G(\omega)$ at $\omega/2\pi = 10$ Hz, we address the question of whether the presence of a phase transition is corroborated also by the frequency dependence of G. This problem is directly related to the validity of dynamical scaling, which is based on the London response for concentration [8–10] as well as thermal [16,17] fluctuations. As in previous experimental [14] and theoretical [16,17] work, we use here instead of G' and G'' the modulus and the phase of $G(\omega)$, which should scale as

$$|G_\pm(\omega)| = G_+(0) S_\pm(\omega/\omega_c(H)),$$
$$\arctan(G''/G') = \phi_\pm(\omega/\omega_c(H)). \quad (1)$$

Near the transition, the characteristic frequency displays the critical slowing down $\omega_c(H) = \omega_0|1 - H/H_{c3}^c|^{\beta\delta}$. In order to check the dynamical scaling, we have extended the $\chi(\omega)$ measurements to the range 1 Hz–1 kHz. The scaled results for $G(\omega)$ are shown in Fig. 3 separately for fields above and below H_{c3}^c. Both modulus and phase fall rather convincingly on two common branches. Since we do not yet have any analytical prediction for the scaling functions, we use, as a crude approximation, the simplest interpolation between both static limits, $G_\pm(\omega \to 0)$, and the critical law $G_c(\omega) = G_c(i\omega/\omega_0)^{-1/2}$,

$$G_\pm(\omega) = [G_\pm^{\mp 1}(0) + G_c^{\mp 1}(\omega)]^{\mp 1}. \quad (2)$$

Regarding the simplicity of this ansatz, containing only the amplitude G_c as free parameter, the agreement for modulus and phase in Fig. 3 turns out to be satisfying.

In order to discuss the nature of the transition, we compare the exponents β, γ, and δ with existing results for thermal and percolation transitions to D-dimensional superconductivity. For the thermal case, passing from our variable $|1 - H/H_{c3}^c(T)|$ to $|1 - T/T_c(H)|$ we insert our exponents into the scaling relation [17] $\delta = 1 + (D - 2)\beta/\gamma$. Then $\beta = \gamma$ and $\delta = 2$ imply $D = \delta + 1 = 3$, inconsistent with $D = 2$ expected for SSC. Therefore, we consider the possibility of percolation for a SC volume fraction $p(H)$ in a D-dimensional network for which $G_+ \sim (p_c - p)^{-s}$ and $G_- \sim (p - p_c)^t$ is expected [8,9].

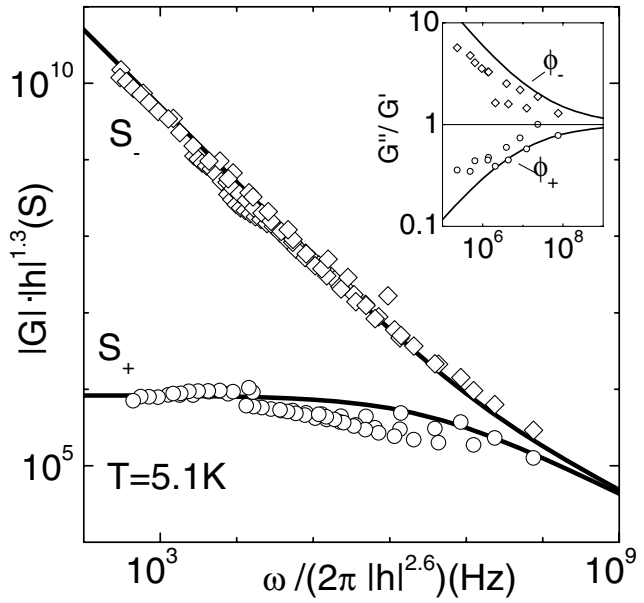

FIG. 3. Dynamical scaling of the modulus and the phase (inset) of $G(\omega)$ between 1 and 900 Hz. The exponents of $h \equiv 1 - H/H^c_{c3}$, contained in both scaling variables, follow from the analysis in Fig. 2. The solid curves are fits to the empirical Eq. (2).

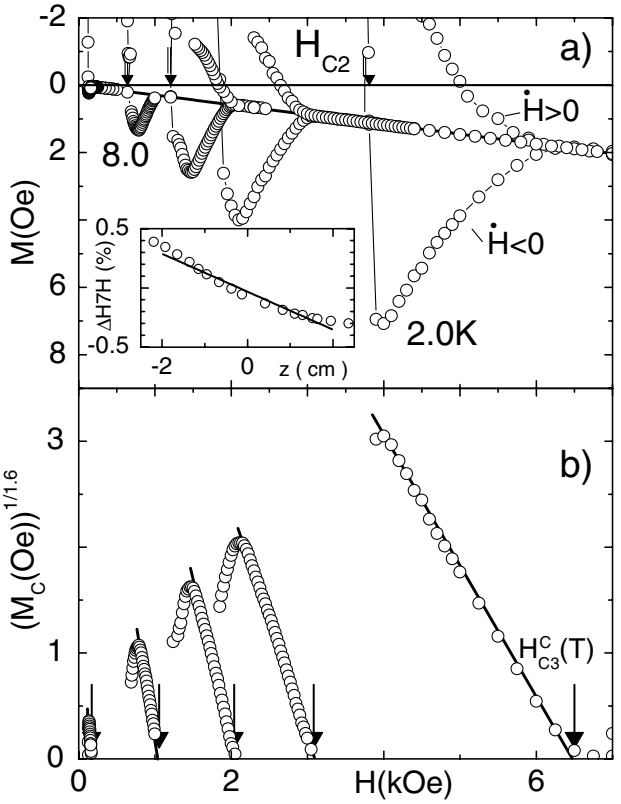

FIG. 4. (a) Magnetization for $H \gtrsim H_{c2}(T)$ recorded at 2.0, 6.0, 7.0, 8.0, and 9.0 K by standard scans of the sample through the weak gradient of the magnet, $\Delta H/\Delta t < 0$. Results from nonstandard (downward) scans, $\dot{H} > 0$, are included for 2–7 K. Inset: Hall-probe results for the gradient, being approximately constant along the 4 cm scan length. (b) Power-law analysis of the ΔH-induced magnetization M_c: straight lines, obtained by a variation of the exponent υ in Eq. (3), terminate exactly at H^c_{c3}.

Similarly, as previous workers [9,18], we utilize near the threshold $p_c = p(H^c_{c3})$ the transformation $p(H) - p_c = |dp/dH|_{H^c_{c3}}(H^c_{c3} - H)$, which allows us to identify $\gamma = s$ and $\beta = t$ with the exponents of the conductivities below and above p_c, respectively. Numerical work yielded $t \cong 1.7$ [8] and $s = 0.74$ [10] for $D = 3$ networks. This is in clear distinction to our results in Fig. 2(b), $\beta = \gamma = 1.3(1)$, which, however, are fully consistent with $s = t = 1.3000$ calculated for $D = 2$ [10]. We consider this outcome as the first and strongest evidence for a percolation-driven transition to coherent SSC.

Some more insight into this novel phase should be provided by the critical current density. For this purpose, we employ the small gradient of the main magnet of our MPMS2, $dH/dz = -10^{-3}H\ \mathrm{cm}^{-1}$ [inset of Fig. 4(a)] directed against the standard scan of the sample through the detection coils. Such a scan consists of 50 steps, each of which induces an electric field along the circumference of the cylinder, $\mathcal{E}_\varphi = (R/2)\mu_0\dot{H}$, depending on the direction and the mean velocity for a single step, $\dot{H} = \dot{z}dH/dz$. The magnetizations are shown in Fig. 4(a) for fields above H_{c2}. As demanded by Lenz's rule, one observes para- and diamagnetic responses, $\pm M_c(H)$, in the standard and nonstandard scan directions, respectively. The linear background magnetization, $\chi_p H$, arises from the normal conducting electrons in the bulk, where $\chi_p = 2.7 \times 10^{-4}$ agrees with earlier reports [19]. We should mention that $M_c(H)$ is independent of increasing and decreasing the static field, except for a very close vicinity of H_{c2} (not depicted in Fig. 4). The other important observation is the independence of $M_c(H)$ on the scan velocity $\dot{z}$, which we varied between 1 and 50 mm/s. This indicates that $\mathcal{E}$ is always large enough to excite the maximum surface supercurrent per unit length of the cylinder, $J_c(H) = M_c(H)$.

In Fig. 4(b), the field variation of the critical current is analyzed in terms of a power law expected for both a thermal, GL-type [20,21] or a percolation transition [22] to SSC. In order to avoid possible correlations between the fitted exponent υ and the onset field for $M_c(H)$, we have varied υ until the low $(J_c(H))^{1/\upsilon}$ values fell on a straight line. By this method we find the onset field to be identical with the coherent surface critical field H^c_{c3}, i.e., the relation

$$M_c(H) = M_c(H_{c2})[(H^c_{c3} - H)/(H^c_{c3} - H_{c2})]^\upsilon, \quad (3)$$

with $\upsilon = 1.6 \pm 0.2$ being independent of temperature. The temperature variations of H^c_{c3} and also of the nucleation field H_{c3} (see Fig. 1) are depicted in Fig. 5. Obviously, both are well described by the variation of $H_{c2}(T)$ [inferred from Fig. 4(a)] defining temperature independent

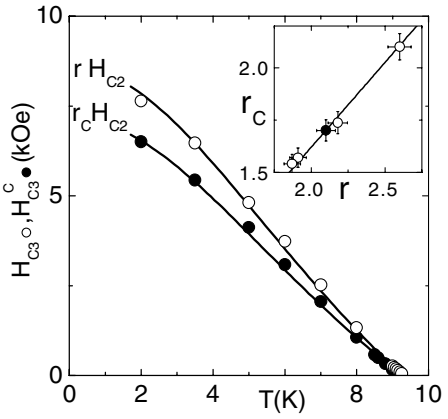

FIG. 5. Nucleation (○) and coherent (●) critical fields, $H_{c3}(T)$ and $H_{c3}^c(T)$. The solid lines show that the temperature dependences are determined by $H_{c2}(T)$. Inset: linear relationship between r_c and r including values from samples with differently prepared surfaces (○) [5].

ratios r_c and r. Both numbers are indicated in the inset of Fig. 5 along with the results from Nb cylinders with larger roughness, different impurity, and grain boundary concentrations at the surface from Ref. [5]. As a challenging result, we find that, despite strong dependence of $r = H_{c3}/H_{c2}$ on the surface structure, the onset of the SSC coherence occurs in all cases at $H_{c3}^c(T) = 0.81H_{c3}(T)$.

By using the same variable transformation as for the analyses of the linear conductance $G' - iG''$ around H_{c3}^c, i.e., $(H_{c3}^c - H) \sim (p - p_c)$, we compare the exponent ν with the scaling prediction for a D-dimensional percolation network, $\nu = t - \Delta$ [22]. The magnitude of the so-called *twistedness* index of the macrobond, Δ, was found to be small and negative for $D = 2$ granular SC PbGe films [22]. This result is fully consistent with our finding $\Delta = t - \nu = (-0.3 \pm 0.3)$ and supports the percolation model. Here, we should note that our result for ν is also close to $\nu = 3/2$ predicted for singly [20] and multiply [21] connected SSC on cylinders. However, these GL-type theories assume $H_{c3}^c = H_{c3}$; i.e., they do not consider the effect of fluctuations, which we have detected in the surface conductance $G' - iG''$ on both sides of H_{c3}^c.

In summary, our analyses of the linear conductance $G(\omega; H, T)$ of a clean Nb cylinder provided clear evidence for a phase transition to coherent SSC at a field $H_{c3}^c(T)$, whereas at the larger, traditional surface critical field, $H_{c3}(T)$, incoherent SSC is nucleated. From the critical behavior of G we conclude that at H_{c3}^c 2D superconducting islands percolate, which is confirmed by the onset of a critical current at H_{c3}^c. As one challenging feature, the ratio $H_{c3}^c(T)/H_{c3}(T) = 0.81$ turns out to be robust against surface roughness and impurities, which, however, have a strong impact on the nucleation field ratio $H_{c3}(T)/H_{c2}(T)$. The latter turns out to be always larger than the classical GL-based ratio $r_{GL} = 1.7$ [1] and deserves also future attention.

We thank B. Steffen, L. Lilje, and P. Schmüser (DESY, Hamburg) for providing the sample, E. H. Brandt (Stuttgart), W. Gil, D. Görlitz, and K. Scharnberg (Hamburg) for useful discussions, and the DFG for a grant to S. C.

[1] D. Saint-James and P. G. de Gennes, Phys. Lett. **7**, 306 (1963).
[2] D. J. Thompson *et al.*, Phys. Rev. Lett. **75**, 529 (1995); P. Kostic *et al.*, Phys. Rev. B **53**, 791 (1996).
[3] M. I. Tsindlekht *et al.*, Phys. Rev. B **62**, 4073 (2000).
[4] S. R. Park *et al.*, Phys. Rev. Lett. **91**, 167003 (2003); X. S. Ling *et al.*, Phys. Rev. Lett. **86**, 712 (2001).
[5] S. Casalbuoni, L. von Sawilski, and J. Kötzler, cond-mat/0310565.
[6] B. Aune *et al.*, Phys. Rev. ST Accel. Beams **3**, 092001 (2000); L. Lilje, Ph.D. thesis, University of Hamburg, 2001 (unpublished).
[7] J. R. Hopkins and D. K. Finnemore, Phys. Rev. B **9**, 108 (1974).
[8] J. P. Straley, Phys. Rev. B **15**, 5733 (1977).
[9] D. Stroud and D. J. Bergman, Phys. Rev. B **25**, 2061 (1982).
[10] J. M. Normand and H. J. Herrmann, Int. J. Mod. Phys. C **1**, 207 (1990).
[11] W. C. Heraeus GmbH & Co. KG, Heraeusstrasse 12-14, D-63450 Hanau, Germany.
[12] Woosik Gil (unpublished).
[13] E. Maxwell and M. Strongin, Phys. Rev. Lett. **10**, 212 (1963); J. R. Clem, H. R. Kerchner, and T. R. Sekula, Phys. Rev. B **14**, 1893 (1976).
[14] J. Kötzler *et al.*, Phys. Rev. Lett. **72**, 2081 (1994); G. Nakielski, Diploma degree thesis, University of Hamburg, 1993 (unpublished).
[15] Since near H_{c3}^c σ is entirely determined by the surface conductance $G = 2R\sigma$, we henceforth refer to G.
[16] D. S. Fisher, M. P. A. Fisher, and D. A. Huse, Phys. Rev. B **43**, 130 (1991).
[17] A. T. Dorsey, Phys. Rev. B **43**, 7575 (1991).
[18] C. J. Lobb, M. Tinkham, and W. J. Skocpol, Solid State Commun. **27**, 1273 (1978).
[19] D. Hechtfischer, Z. Phys. B **23**, 255 (1976).
[20] A. A. Abrikosov, Sov. Phys. JETP **20**, 480 (1965).
[21] H. J. Fink and L. J. Barnes, Phys. Rev. Lett. **15**, 792 (1965).
[22] G. Deutscher and M. L. Rappaport, J. Phys. (Paris), Lett. **40**, L219 (1979).